CHAPTER 5

Pigments on a tile from the Citadel of Algiers

The analysis and detailed characterisation of pigments on artworks and other materials of archaeological origin has become increasingly indispensable in the identification, authentication and restoration of these important artifacts and can lead to more effective conservation plans, thus preserving the artifacts for posterity. In the case of the tile from the Citadel of Algiers, the information could also be used to rebuild and restore the Citadel to its former pre-colonial state. This chapter therefore deals with the study of pigments on this tile shard. This tile shard was selected because, apart from its obvious historical significance, it has a predominantly SnO_2-based glaze. The glaze depth profile method that allows for the study of ceramic/glaze interfacial pigments on intact porcelain artifacts, as successfully used in Chapter 4, was applied to this tile shard as well, partly to validate the method and also to gather useful information on the shard. Some of the information presented in this chapter has been published in *Spectrochimica Acta Part A: Molecular and Biomolecular Spectroscopy*.[1]

5.1 Tile history and description

The multi-coloured tile shard under study (see Figure 5.1.1) was obtained from the Citadel of Algiers.[2] The various colours are defined qualitatively for discussion purposes starting with the heterogeneous shades of yellow (bright yellow, orange yellow and brown yellow). The other colours are blue, white, reddish brown (line) and brown-black (line).

Figure 5.1.1. The different views of the Citadel tile highlight the different colours (above) and the relative thickness of the tile body (below) with respect to the glaze thickness

The tile shard body is composed mainly of brown material which will also be discussed in detail in this chapter. The white pigment on the tile forms the base on which all the other pigments are spread, in addition to the white surface sections which form part of the decoration (Figure 5.1.1).

The following is an extract from a French translation describing the origin of the tile and giving a short history of the Citadel of Algiers, obtained from the donor of the tile shard.[2]

THE CITADEL OF ALGIERS
TRANSLATION FROM THE FRENCH

"Situated at 118 metres above sea level, the Citadel of Algiers stood above the Medina (Temple) of El Djezair on the south-western side and formed the sloping angle from where the ramparts of the Medina ran downwards towards the sea.

"Started in 1516 on the instructions of Aroudj Barbarossa and enlarged by Mustapha Pasha, the Citadel was originally a military fortress until 1817, the year in which the second-last Dey (ruler) Ali Khodja decided to turn it into his residence and the seat of his government.

"On the arrival of the Dey Hussein as the head of government, the Citadel was rearranged in terms of its new function – that of seat of administration, justice and finance. It consisted of:

- The Palace of the Dey and its outbuildings, at the time divided into a wing reserved for women, apartments for the Dey, meeting halls for the council, kitchens and store rooms
- The mosque of the Dey, reserved for the Dey and his officials
- The palace and baths of the agha
- The palace of the Beys (regional rulers?) and its outbuildings reserved for the Beys of Constantinople, Medea and Oran, who came every three years for the Douches (tribute payable to the Beylik (Chief Dey) by these three provinces)
- The mosque of the guards
- The gunpowder room, which served for the manufacturing of saltpetre and which today is the only architectural example of its kind in Algeria
- The distribution of water

- The gardens (winter and summer)
- The ostrich park
- Five sets of cannons
- The bunkers housing the guards

"Converted into barracks from the start of the French colonisation in 1830, the Citadel was inhabited by the generals of this army until 1840, during which year certain sectors were changed into a military hospital. Classified as a historical monument as from 1887, a section of the Citadel (the palace of the Dey, the mosque of the Dey and the gunpowder room) was converted into a colonial military museum in 1930. With the independence of Algeria in 1962, the entire contents of the museum were removed by the French.

"Today the Citadel is being restored and developed in order to return this historical complex, symbol of the Algerian state before colonisation, to its erstwhile importance".[2]

(Supplied by the donor of the tile shard from the Citadel of Algiers)

5.2 Pigment analysis on the Citadel tile

The method of tile pigment analysis that was followed included micro-Raman spectroscopy, X-ray powder diffraction (XRD), Energy dispersive X-ray spectrometry (EDX) and a separate synthesis of related reference compounds to aid in the Raman band assignments and XRD studies.

5.2.1 Yellow pigments

It must be noted that lead-based yellow pigments have been in use[3] since 1600. Among the earliest that are known to have been used are the following: lead (II) stannate (Pb_2SnO_4), lead (II) antimonate, often called Naples yellow ($Pb_2Sb_2O_7$), and lead (II) oxides (orthorhombic and tetragonal).[3] Despite the fact that these pigments were widely manufactured and used, some of the ancient recipes are not well understood or even known. The detailed study of these ancient pigments is further complicated by the use of less-than-pure starting materials that were peculiar to the areas from which the raw materials were obtained. Table 5.2.1.1 is a summary of these ancient yellow pigments as adapted from the work of Clark.[3]

Table 5.2.1.1. Summary of the ancient yellow pigments and some of the Raman band assignments (adapted from Clark[3])

Compound	λ_o / nm	Wavenumber / cm^{-1}
Pb_2SnO_4	514.5	35wm, 58w, 80m, 129vs, 196m, 274w, 291wm, 379w, 454wm, 524w, 613w,
Pb_3O_4	647.1	121vs, 152m, 223w, 232w, 313w, 391w, 477w, 549s.
$PbSn_{1-x}Si_xO_3$	514.5	40m, 66m, 85(sh), 138vs, 324wm(br), 444w (br).
$Pb_2Sb_2O_7$	514.5	76s, 147vs, 343s, 464m, 513wm,
PbO (massicot orthorhombic, yellow)	647.1	87s, 144vvs, 171(sh), 217vw, 289vs, 385m, 424w.
PbO (Litharge tetragonal, reddish)	647.1	81s, 147vvs, 322vw, 338s

It has been noted that the most common of these yellow pigments have a dominant Raman band at ca 127-145 cm^{-1} and differ from each other by the position of this dominant band (DB) which has been attributed to a Pb-O stretching mode.[3] The following differences in the position of this dominant Raman band can be found in these common pigments: lead tin yellow [type I (DB at 129 (vs) cm^{-1} and 196 cm^{-1} (s)) and type II (DB at 138 cm^{-1} (vs) and broad bands at 324 cm^{-1} (m)], lead (II) antimonate [DB at 140 cm^{-1} and broad bands at 329 cm^{-1} (m) and 442 cm^{-1} (w)], two lead (II) oxides [orthorhombic (143 cm^{-1} (vs), 289 cm^{-1} (s) and 385 cm^{-1} (w)] and tetragonal [145 cm^{-1} (vs), 285 cm^{-1} (vw) and 336 cm^{-1} (vw)] crystals.[3]

On the basis of this introductory information, the yellow pigment on the tile has been studied, identified and characterised.

5.2.1.1 Ancient rediscovered yellow pigment ($Pb_2SnSbO_{6.5}$)

Representative Raman spectra of the yellow pigment on the Citadel tile were acquired at many different locations on the tile. The three distinct spectra that were obtained all differed from well-known ancient yellow pigments such as lead tin yellow types I and II, lead antimonate yellow, Naples yellow and other related pigments.[3,4-6] Interest was not focused exclusively on the Pb-O dominant Raman vibration since it had already been shown that these compounds by and large differ by the position of this band.[3] Instead, interest was focused on the entire Raman spectrum within the collected region of 100 cm^{-1} to 1300 cm^{-1}.

It was found that the yellow pigment on the tile is fairly similar to another ancient yellow pigment (pyrochlore type) which was recently identified on Italian paintings of the 16th century by G.B. Langetti (“Lot and his daughters”) and Luca Giordano (“Entrance of Christ in Jerusalem”)[7] and on Italian pottery of the 16th century.[8,9] This

pigment can be described as a pyrochlore-type ternary system represented by the formula $Pb_2SnSbO_{6.5}$.

Figure 5.2.1.1.1 shows the Raman spectra collected from the yellow sections according to the shade of yellow pigment, using 568 nm wavelength radiation. It is also noted that a similar trend was observed using the 514.5 nm wavelength radiation, showing that the 127 cm^{-1} Raman band is associated with the ternary compound $Pb_2SnSbO_{6.5}$.

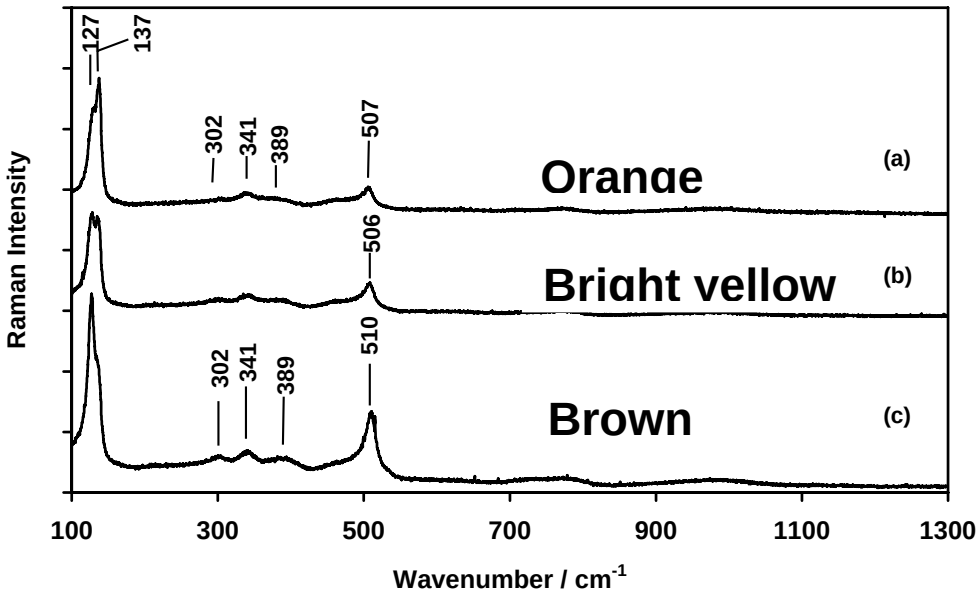

Figure 5.2.1.1.1. This Figure shows spectra of the various shades of yellow pigment with 568 nm wavelength radiation at 0.5 mW at the sample. The wavenumber resolution is 2 cm^{-1}

Since these spectra are similar to the literature assignments but not conclusive, the first task was to determine which spectra among them correspond to this ternary compound and to which pigments the other spectra correspond.

It must also be noted that the literature assignment for the Pb-O Raman band for this ternary yellow pigment ($Pb_2SnSbO_{6.5}$) is placed at 132 cm^{-1}; it is sometimes indicated as 127 cm^{-1} – 137 cm^{-1} and is shown as a doublet in this region.[7-10] In this study, three distinct phases (by colour) corresponding to bright yellow, brown-yellow and an orange-yellow making up the yellow section of the Citadel tile were observed. Using the synthesis methods described by Cascales and co-workers[10] for these types of pyrochlore system, several reference samples were synthesised, as described in Chapter 3. XRD data were collected for these samples, as shown in Table 5.2.1.1.1.

Table 5.2.1.1.1. XRD results for synthesised samples, labelled from (a) to (e) according to the ratio of Pb to Sn to Sb (Pb:Sn:Sb)

Sample	Ratio Pb:Sn:Sb	XRD results
(a)	2:1:1	$Pb_2SnSbO_{6.5}$ (dominant) $PbSb_2O_6$ (trace) SnO_2 (starting material)
(b)	Excess Sb	$Pb_{3+x}Sb_2O_{8+x}$ Sb_2O_4 (starting material) $PbSb_2O_6$
(c)	Excess Sn	$Pb_2SnSbO_{6.5}$(trace) Pb_2SnO_4 SnO_2 (starting material)
(d)	2:1:0	Pb_2SnO_4 (dominant)
(e)	2:0:1	$PbSb_2O_6$ (dominant)

The following discussion relates the synthesised pigments to those on the Citadel tile. The use of Raman spectra in conjunction with XRD data for samples (a) and (e) revealed that the dominant Pb-O Raman band for the ternary pyrochlore-type pigment ($Pb_2SnSbO_{6.5}$) is at 127 cm^{-1} rather than at the 132 cm^{-1} reported in the literature.[7-9] Figure 5.2.1.1.2 is the Raman spectrum of the synthesised pigment resulting from starting materials containing Pb:Sn:Sb = 2:1:1.

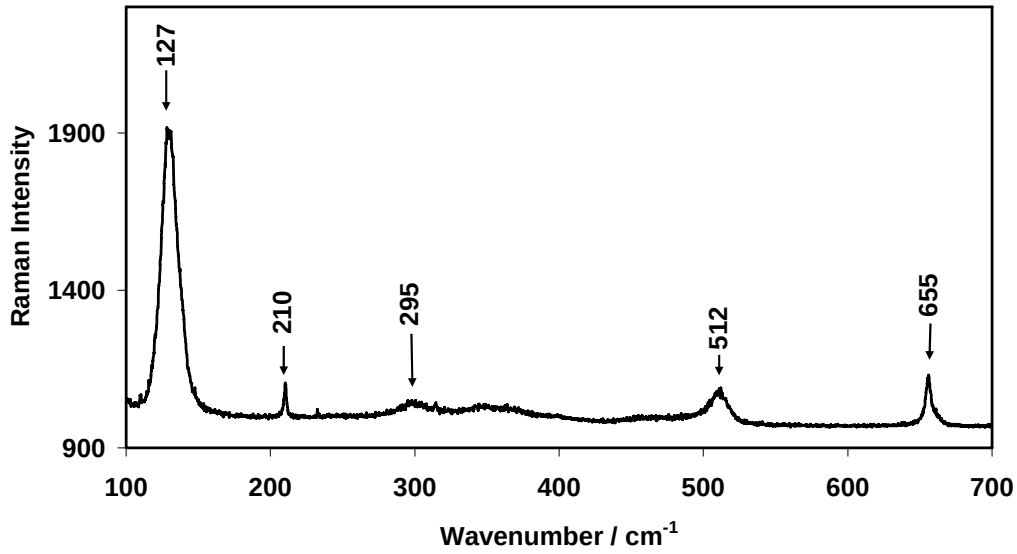

Figure 5.2.1.1.2. Raman spectrum of sample (a) in Table 5.2.1.1.1. The Raman bands at 210 cm^{-1} and 655 cm^{-1} are assigned to trace amounts of rosiaite ($PbSb_2O_6$). A 514.5 nm wavelength radiation, 0.3 mW laser power at the sample, with 2 cm^{-1} wavenumber resolution was used

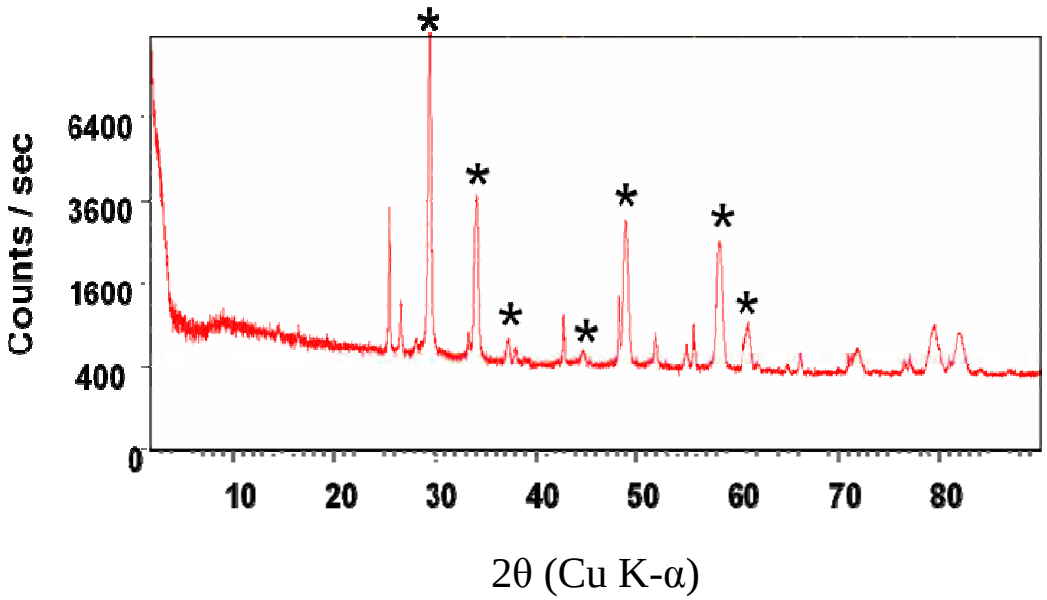

Figure 5.2.1.1.3. The XRD pattern of sample (a) in Table 5.2.1.1.1, shows the ternary pyrochlore as the dominant product. The asterisks are used to show the ternary compound ($Pb_2SnSbO_{6.5}$)

This spectrum was compared with those of the various yellow pigments on the tile shard (Figure 5.2.1.1.1). The literature spectrum of the ternary pigment ($Pb_2SnSbO_{6.5}$) is reported by Ruiz-Moreno and co-workers[7] and Sandalinas and co-workers[8,-9] to sometimes have a doublet at 127 cm^{-1} and 137 cm^{-1}. A comparison with the product prepared in this laboratory, with a ratio of Pb:Sn:Sb = 2:1:1 presumed to be this ternary pigment, shows only one single band at 127 cm^{-1}.

In order to verify whether the prepared pigment is indeed the ternary compound $Pb_2SnSbO_{6.5}$, an XRD spectrum was obtained and indeed the XRD data for the synthesised sample shown in Figure 5.2.1.1.3. do indicate that the ternary pigment $Pb_2SnSbO_{6.5}$ is the dominant component, with small amounts of rosiaite ($PbSb_2O_6$).

The Raman bands at 210 cm^{-1} and 655 cm^{-1} that are also present in Figure 5.2.1.1.2. are attributed to $PbSb_2O_6$ (rosiaite). A compound prepared with Pb:Sn:Sb = 1:0:2, as in Table 5.2.1.1.1 row (e), was confirmed to yield $PbSb_2O_6$ (rosiaite) as a dominant product. The Raman spectrum of the synthesised rosiaite (Table 5.2.1.1.1 row (e)) is shown in Figure 5.2.1.1.4. As expected, the two Raman bands attributed to rosiaite at 210 cm^{-1} and 665 cm^{-1} are now most intense, confirming that the product in Table 5.2.1.1.1 row (e) is indeed $PbSb_2O_6$ (rosiaite). The XRD results of the synthesised rosiaite as shown in Figure 5.2.1.5 also confirm that the dominant compound in the synthesised sample of Table 5.2.1.1.1.(e) is indeed rosiaite.

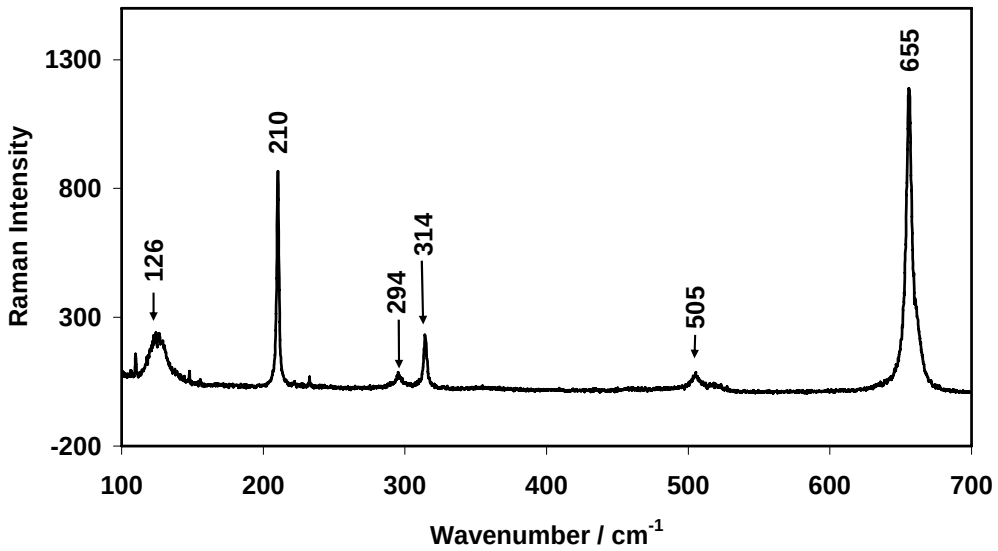

Figure 5.2.1.1.4. The Raman spectrum of sample (e) in Table 5.2.1.2. is consistent with the XRD data. This sample shows two sharp Raman bands at 210 cm^{-1} and 655 cm^{-1} characteristic of $PbSb_2O_6$, in addition to the other Raman bands.

In addition to rosiaite ($PbSb_2O_6$), an unknown component ($Pb_{3+x}Sb_2O_{8+x}$) was also detected in the product (see also sample (b), Table 5.2.1.1.1). The XRD pattern (Figure 5.2.1.1.5) is also consistent with the Raman results

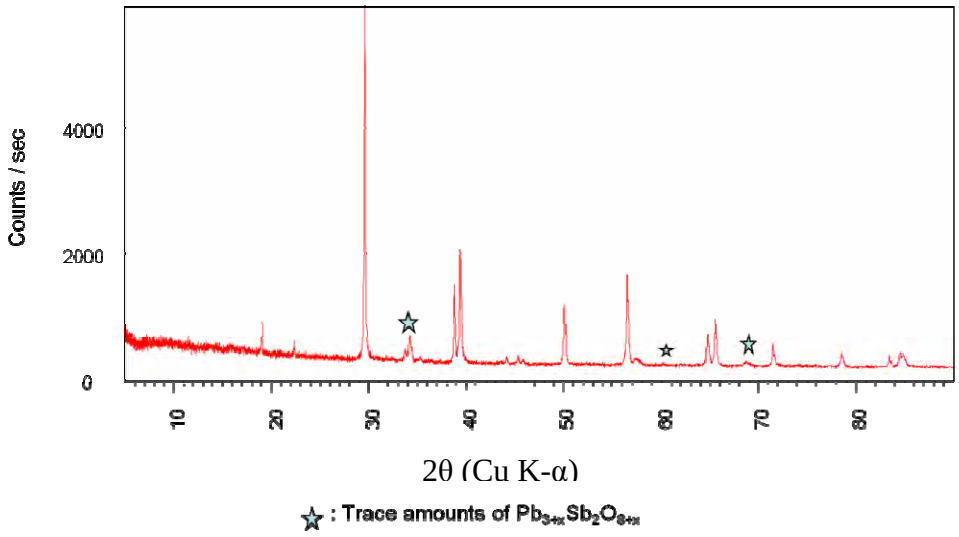

Figure 5.2.1.1.5. XRD pattern of the synthetic rosiaite ($PbSb_2O_6$) with trace amounts of the unknown compound $Pb_{3+x}Sb_2O_{8+x}$ indicated with a star

Figure 5.2.1.1.6 shows the Raman spectrum of a compound prepared with a ratio of Pb:Sn:Sb = 2:1:0 (no antimony), identified as Pb_2SnO_4.

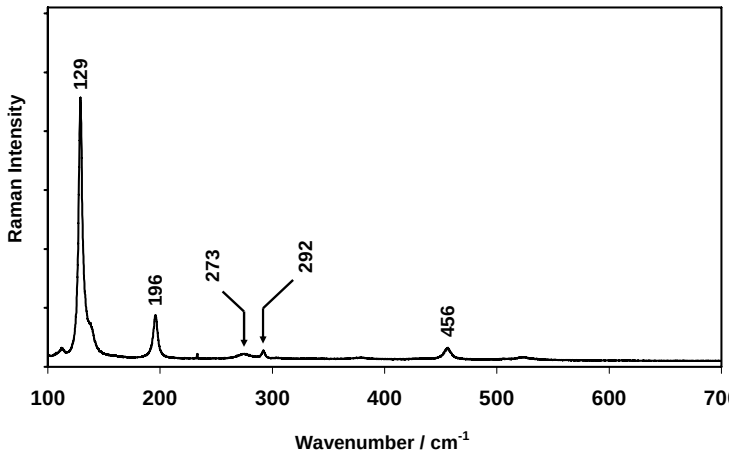

Figure 5.2.1.1.6. Raman spectrum of sample (d) in Table 5.2.1.2, consistent with Pb_2SnO_4 (see also row one of Table 5.2.1.1 from Clark[3] for the Raman band assignments for this compound)

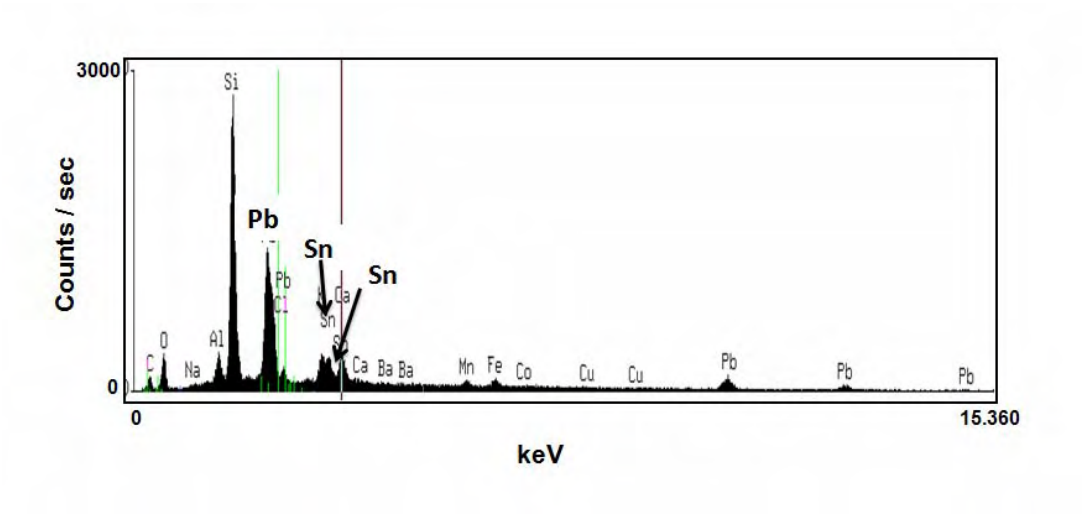

Figure 5.2.1.1.7. EDX spectra of the brown line on the Citadel tile. The ratio of Pb:Sn = 2.19 is close to that of Pb_2SnO_4. The sample penetration depth is in the order of 20 µm

This compound also appears as the dominant component in a sample prepared with an excess of tin over antimony (see Figure 5.2.1.1.1). The ternary compound ($Pb_2SnSbO_{6.5}$) and the starting material (SnO_2) also appear as trace components. This information points to the dominant Pb-O Raman band for this sample being around 129 cm^{-1}.

It is therefore concluded that the compound prepared according to a Pb:Sn ratio of 2:1 in Table 5.2.1.1.1(c) is lead (II) stannate (Pb_2SnO_4). It must be noted that the EDX results also depend on the beam penetration into the glaze and may give larger errors due to underlying material. The large amount of silicon in Figure 5.2.1.1.7 is due to the underlying glaze. The Raman results for lead (II) stannate on the Citadel tile show a mixture of pigments that can be assigned to the lead tin yellow type II ($PbSn_{1-x}Si_xO_3$) shown in Figure 5.2.1.1.8.

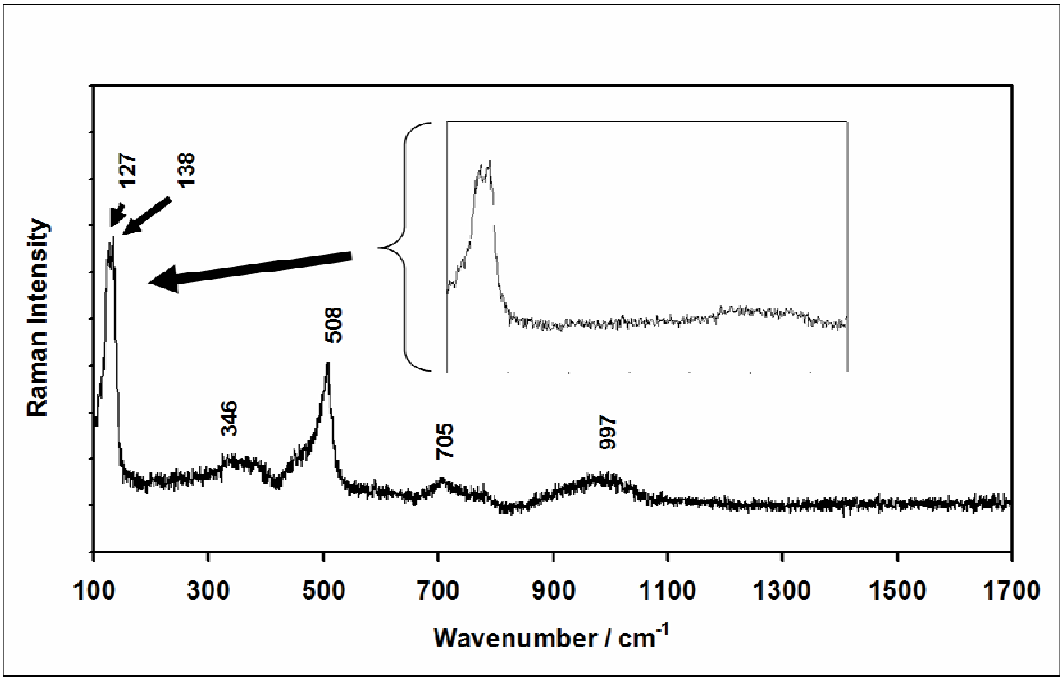

Figure 5.2.1.1.8. Raman spectrum of the tile pigment showing the presence of lead tin yellow type II ($PbSn_{1-x}Si_xO_3$) on the tile shard

It is therefore concluded that the ternary pyrochlore ($Pb_2SnSbO_{6.5}$) on the tile shard is the brownish yellow pigment with the dominant Pb-O vibration at 127 cm^{-1} and not the bright yellow pigment normally found on Italian paintings of the 16th century with its dominant Pb-O Raman band at 132 cm^{-1}. It appears that this bright yellow pigment consisted of mixtures of pigments, including the ternary pyrochlore structure ($Pb_2SnSbO_{6.5}$) and tin-rich lead stennate (Pb_2SnO_4). These mixtures sometimes contained silica and even rock salt as flux to produce the desired hue.[7]

EDX data were obtained for the different sections of the tile pigments. Although EDX data may not be accurate due to the possibility of including up to 20 µm of underlying sections, they can nevertheless, be an estimate of the element ratios on the various colour backgrounds on the Citadel tile. Typical EDX results are shown in Appendix 5.1.

5.2.1.2 Naples yellow or lead antimonite ($Pb_2Sb_2O_7$)

Naples yellow or lead antimonate yellow ($Pb_2Sb_2O_7$) is the most common of the yellow pigments used by the western European artists[11] from about 1500 to 1850. The identification of this pigment on a tile from the Citadel of Algiers produced in 1516 indicates the availability and use of this pigment in the Mediterranean region very early on during this period. This may support the assertion that this pigment originates from the Middle Eastern ceramic and glass industries of the 15th century and that the know-how on the production of lead antimonite yellows was transferred via the migration of glass artists from the eastern Mediterranean to Venice during the 15th century.[11] Figure 5.2.1.2.1 shows the Raman spectrum of the reddish-brown yellow pigment on the tile shard. The two strong Raman bands at 140 cm^{-1} and 510 cm^{-1} are consistent with literature assignments for Naples yellow.[12]

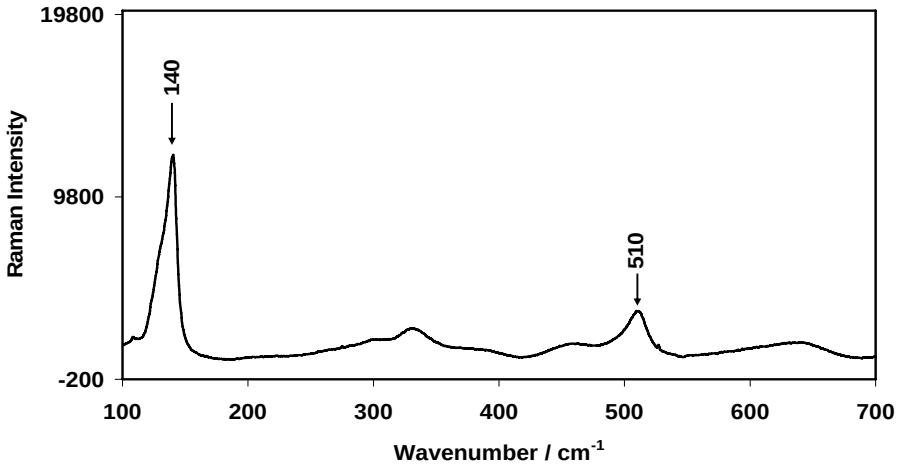

Figure 5.2.1.2.1. Naples yellow Raman spectrum as identified on the Citadel tile. The wavelength of the excitation line was 514.5 nm and the power at source was 0.5 mW

The EDX results obtained directly on this pigment from the tile shard also show ratios of Pb:Sb = 1:1. These ratios are determined by noting that the weight

percentages given by EDX results are simply averages of atomic concentrations in the path of the beam and can therefore be used to determine the approximate ratios of atoms using the same data set. These results are also consistent with the formula $Pb_2Sb_2O_7$ that has been determined for Naples yellow.[3] Figure 5.2.1.2.2 is representative of the EDX spectra that were used to generate the table in Appendix 5.1, in this case for the white section of the tile shard.

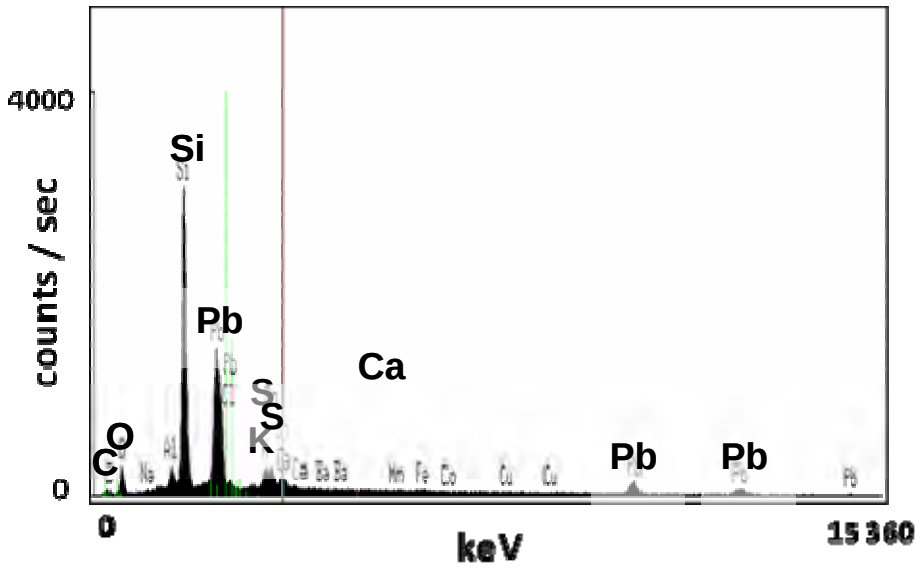

Figure 5.2.1.2.2. Representative EDX spectra on the white section of the tile. Similar EDX spectra and associated information where used to generate tables, such as that of Appendix 5.1

5.2.1.3 White pigment: cassiterite (SnO_2)

The glaze on the Citadel tile is composed largely of cassiterite (SnO_2). Raman spectra from this white pigment shown in Figure 5.2.1.3.1(a) were compared with those of a reference compound (Figure 5.2.1.3.1(b)) purchased from Merck, Johannesburg. The cassiterite structure belongs to the tetragonal crystal system with two molecules per unit cell, $P_{4/2mnm}$ (D^{14}_{2h}) space group.[13-14]

From consideration of group theory, four Raman-active bands are given as A_{1g}, B_{1g}, B_{2g} and E_g. Two of the Raman bands that are observed (Figure 5.2.1.3.1) may be assigned as the 635 cm^{-1} (A_{1g}) and 799 cm^{-1} (B_{2g}) Raman bands.[15] Due to the broad bands around 500 cm^{-1} and 1000 cm^{-1}, the cassiterite Raman band around 513 cm^{-1} observed in the reference spectrum is not observed in the tile spectrum. However, the two Raman bands observed and their relative intensity are sufficient to identify this white pigment as cassiterite (SnO_2).

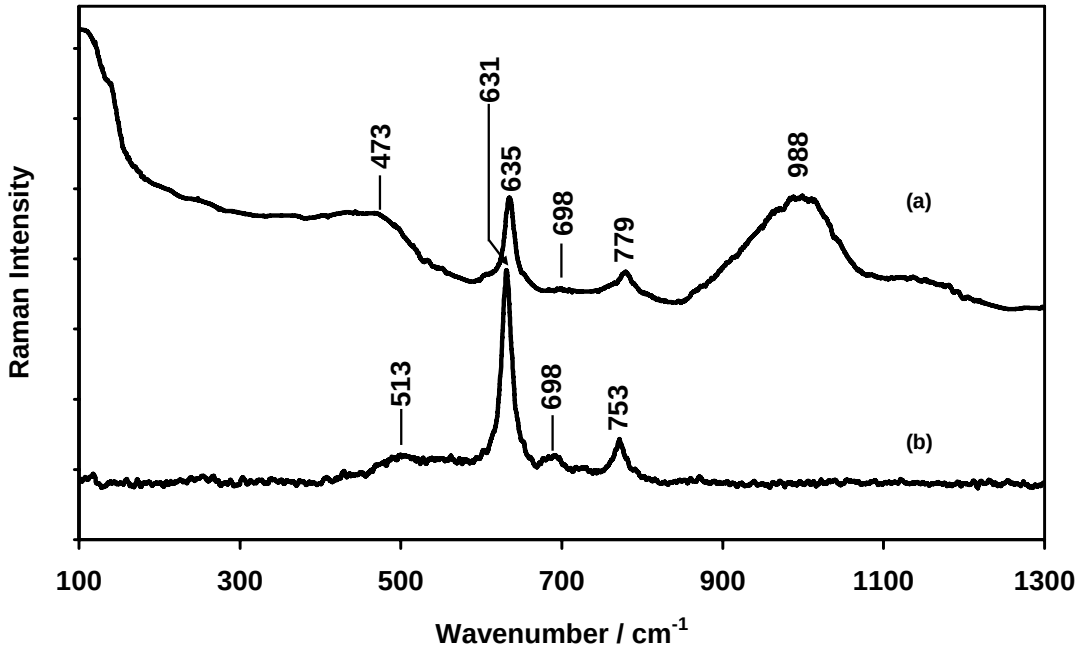

Figure 5.2.1.3.1. Two Raman bands for white pigment: the spectrum in (a) is that from the white pigment on the Citadel tile and (b) is that of a reference compound SnO_2

Historically, cassiterite was used as an opacifier[15] and in some instances it has been found mixed in with α-quartz in ceramic materials from the period 1510–1530 in Iznik (former Nicaea).[16] It is conceivable that this was also the intention here since the Citadel of Algiers was built in 1516. Using the glaze depth profiles generated by

Raman spectra, it was possible to show that some amorphous carbon is found inside the glaze of the tile and not on the surface of the tile as indicated in Figure 5.2.1.3.2. In this figure, the top spectrum (a) is that collected at the surface of the glaze (0 µm), while the bottom spectrum (e) was collected at 30 µm inside the glaze. It is also concluded that this amorphous carbon may be due to contamination at the time of manufacture of the Citadel tile.

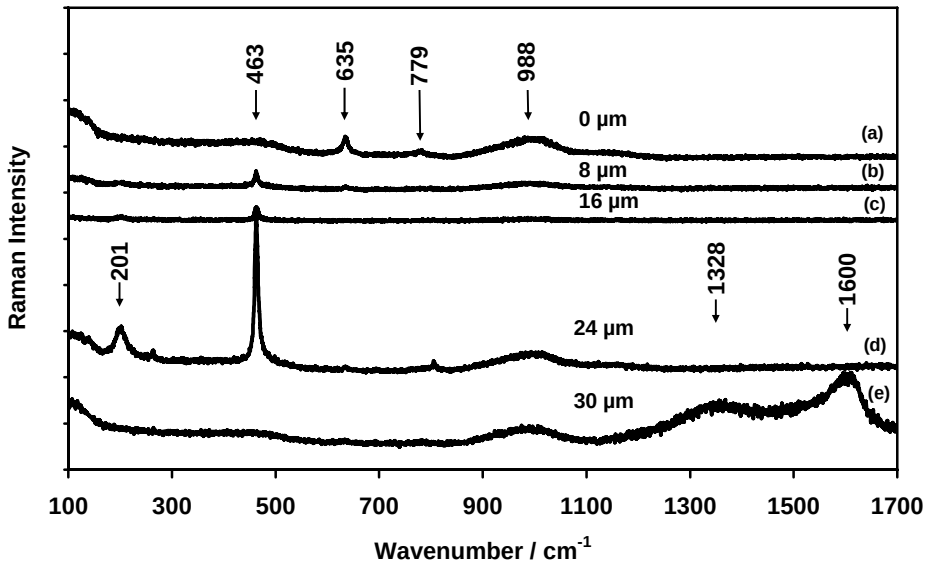

Figure 5.2.1.3.2. Glaze depth profile spectra generated on the white background of the Citadel tile, also showing amorphous carbon at a depth of 30 µm

5.2.1.4 Blue pigment: cobalt aluminium oxide ($CoAl_2O_4$)

Figure 5.2.1.4.1 shows a high-resolution picture (100X magnification) of the blue background on the glaze of the Citadel tile shard. The blue pigment is seen to be spread homogeneously through the glaze. However, repeated glaze depth profile Raman spectra on the blue background did not reveal the identity of the blue pigment. Figure 5.2.1.4.2 shows this profile and reveals only cassiterite and quartz.

Figure 5.2.1.4.1. The cross-section of the blue background from the tile shard is shown. The blue pigment is shown spread homogeneously through the top section of the tile shard and could be the result of dissolved cobalt

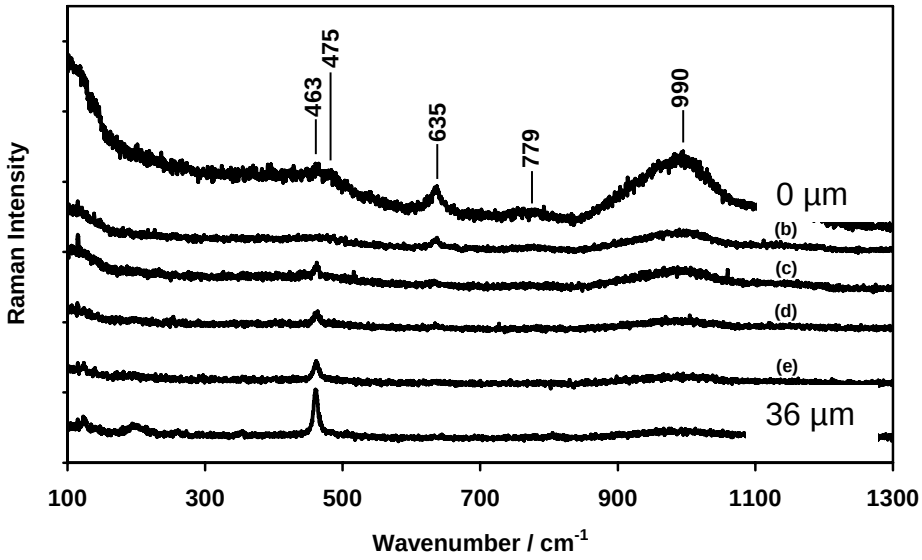

Figure 5.2.1.4.2. Glaze depth profile Raman spectra, which does not show the identity of the blue colour but shows that cassiterite and quartz form part of the glaze However, it has been shown elsewhere[17] that dissolved cobalt can give a distinct blue colour while remaining undetected.

It is customary to use the concept of scattering cross-section when scattering efficiencies are considered. In the case of the cobalt entity in the glaze of the tile, we sought only to show that due to low scattering efficiency and the small scattering cross-section, this cobalt entity in the tile glaze may be undetected. The Raman signal intensity depends on a number of factors, among which are the following: molecular density (ρ); sample thickness; and the first differential Raman cross-section ($d\sigma/d\Omega$), which is itself dependent on the excitation radiation to the inverse fourth power ($1/\lambda^4$), where $d\Omega$ is the solid angle defining the scattered photon flux.

The proportionality of the Raman signal intensity can be represented by the following expression:[18,19]:

$$\frac{d\sigma}{d\Omega} \times \rho \times \int_0^D 1_0^{-(\alpha_0+\alpha_R)dr} \qquad 5.1$$

where

$\frac{d\sigma}{d\Omega} \equiv$ differential Raman cross-section

$\alpha_0 \equiv$ absorptivity at a reference wavelength

$\alpha_R \equiv$ absorptivity at the Raman line

$\rho \equiv$ molecular density

$D \equiv$ sample thickness

where the triple lines indicate equivalency.

Firstly, despite the intense bright blue colour on the tile, the molecular density could be very low. Secondly, sample thickness in the glaze is in the order of < 1 µm due to the use of confocal Raman configuration. Thirdly, the first differential Raman cross-sections ($d\sigma/d\Omega$) are in the order of $\approx 10^{-31} - 10^{-28}$ cm^2 sr^{-1} and there are therefore lower limits of detection for Raman spectroscopy.[20] Therefore, if the pigment concentration in the glaze is orders of magnitude smaller than the lower limits, for example comparable to molecular mono-layers within the sampled volume, then the pigment in the glaze will be undetectable without any form of signal enhancement such as surface enhanced Raman spectroscopy (SERS) or resonance effects. For instance, silver nanocrystals could have been spread on the surface of the glaze to come into contact with the surface, in which case a Raman spectrum of the surface in contact with the silver particles would be obtained. Alternatively, the transparency to Raman spectroscopy of the blue colour in this glaze could be the result of dissolved cobalt ions in the glass structure.[17]

However, a small amount of pigment was detected in crevices in the glaze and a spectrum was recorded and identified as cobalt blue or cobalt aluminium oxide.[21] Due to the fact that cobalt blue was not directly observed in the bulk of the glaze using Raman spectroscopy, it may be advisable to conduct further research using other techniques to identify conclusively the exact cobalt structure that is giving rise to this beautiful blue colour in the glaze (Figure 5.2.1.4.1).

5.3 Tile body analysis

The body of the tile appears red/brown in colour but appears to be rather heterogeneous with black, red/brown and white particles showing under the microscope. These particles were analysed directly using low-power radiation (5 mW of 514.5 nm radiation at the source). The chemical composition of the tile body will now be discussed.

5.3.1 Iron oxides

5.3.1.1 Hematite (α-Fe_2O_3)

Figure 5.3.1.1.1 (a) shows the Raman spectrum collected from the black/brown particles on the tile body. The observed spectrum is shown to be that of hematite. All seven Raman-active bands of hematite that are predicted by group theory ($2A_{1g}$ + $5E_g$) were observed. The assignment of these Raman bands follows directly from the literature[22] as 226 cm^{-1} (A_{1g}), 247 cm^{-1} (E_g), 292 cm^{-1} (E_g), 411 cm^{-1} (E_g), 607 cm^{-1} (E_g) and 496 cm^{-1} (A_{1g}), and the magnon band observed at 1330 cm^{-1}. The 298 cm^{-1}(E_g) is seen only as a shoulder on the 292 cm^{-1} band (Figure 5.3.1.1.1(a)), consistent with observations in other studies.[22,23]

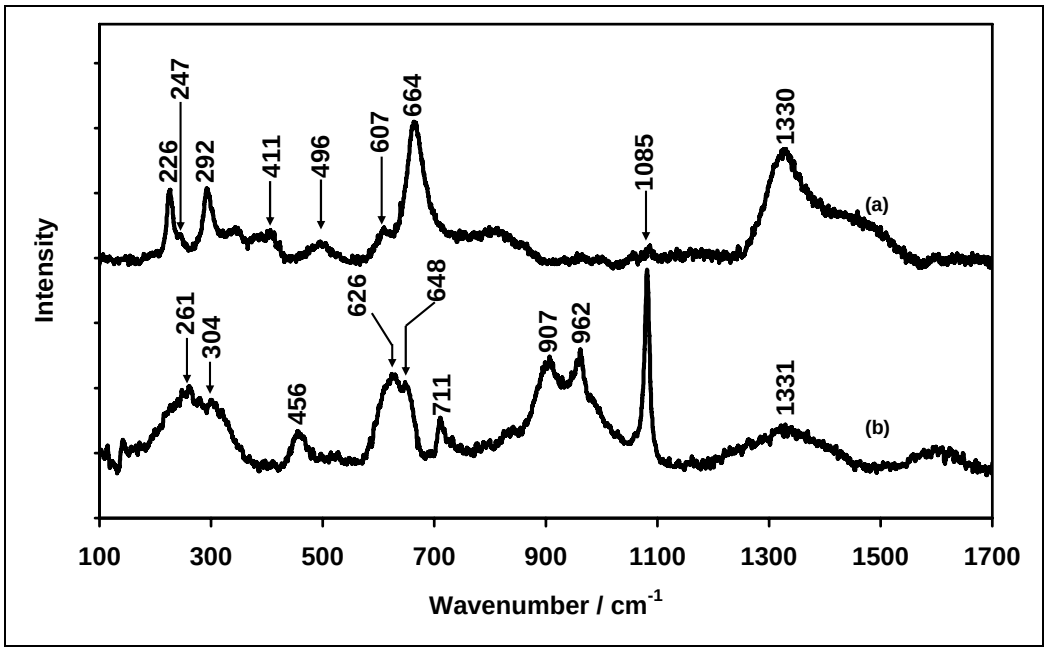

Figure 5.3.1.1.1. The presence of hematite (α-Fe_2O_3) is indicated by the observation of all the hematite Raman bands in Figure 5.3.1.1.1(a)

5.3.1.2 Maghemite (γ-Fe_2O_3)

Maghemite (γ-Fe_2O_3) has an inverse spinel structure which appears as an Fe-deficient form of magnetite.[16] However, its Raman spectrum is not well defined[24] and it is known to be characterised by broad features around 350 cm^{-1}, 500 cm^{-1} and 700 cm^{-1} as can also be seen in this study (Figure 5.3.1.1.1(b)). It must be noted that the broad features identified in the maghemite spectrum are not present in any of the other iron oxides or oxyhydroxides[25] that are usually found in clays.

5.3.1.3 Magnetite (Fe_3O_4)

The presence of magnetite (Fe_3O_4) in the body of the tile could have come from the raw material that was used. Magnetite occurs naturally in clay bodies[25] and its presence in the tile would not be a surprise if it is assumed that the raw material was a naturally occurring clay. Indeed, Figure 5.3.1.1.1(a) shows a relatively strong Raman band at 664 cm^{-1} that is not part of the α-Fe_2O_3 spectrum. No other iron oxide shows this Raman band, except würzite (FeO), in which it is usually broad and shifted to lower wavenumbers.[23] This phase is therefore attributed to magnetite.[26]

5.3.2 Quartz (α-SiO_2)

Two forms of quartz were identified on the tile. Figure 5.3.4.1(b) shows a strong A_{1g} mode of α-SiO_2 at 464 cm^{-1} and a broad Raman band attributed to glassy silica at 459 cm^{-1}.

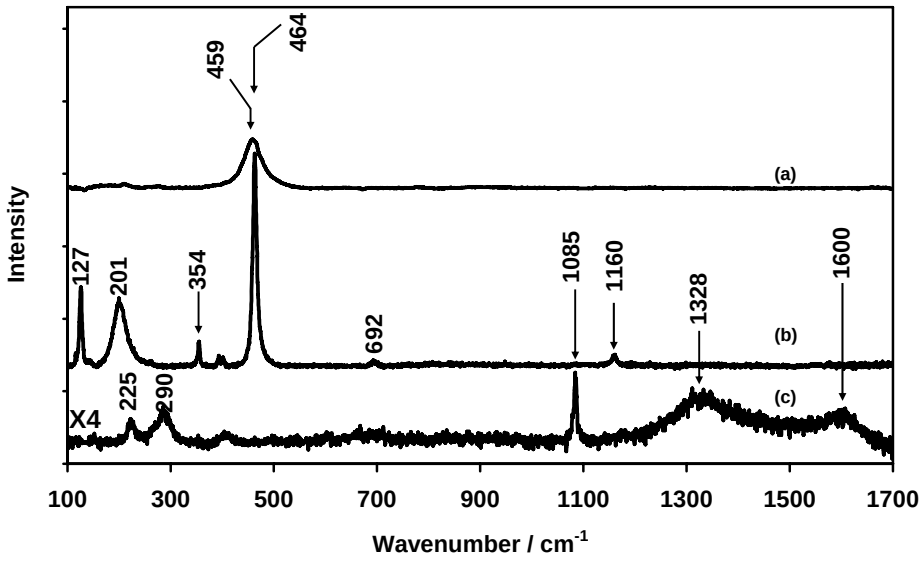

Figure 5.3.4.1. Both glassy silica (a) and quartz (b) were detected on the body of the tile. Amorphous carbon and traces of calcite were also detected as shown in (c)

These phases appear as white crystalline materials embedded in the body of the tile and may have been part of the original material of manufacture of the tile.

5.3.3 Calcite ($CaCO_3$)

Calcite ($CaCO_3$) was detected in the body of the Citadel tile and is identified by the two Raman bands at 1085 cm^{-1} (A_{1g}) and 711 cm^{-1} (E_g)[27,28] (see Figure 5.3.1.1.1(b)). There are two other forms of $CaCO_3$ and both show a strong Raman band around 1085 cm^{-1}. However, these two other phases (aragonite and vaterite) also show additional Raman bands at 700 cm^{-1} and 750 cm^{-1}, respectively.[27] Therefore the phase in the body of the tile is positively identified as calcite.

5.3.4 Amorphous carbon

The glaze of this tile did not show any presence of amorphous carbon on the surface, except for trace amounts inside the glaze (Figure 5.2.1.3.2(e)) and the body of the tile (Figure 5.3.4.1(c)). The amorphous carbon detected in both cases is presumed to be due to accidental contamination during the manufacture of the tile. This contamination is identified by two broad bands around 1350 cm^{-1} and 1600 cm^{-1} and these bands are associated with the "D" and "G" Raman bands of graphitic carbon.[29,30] A high-resolution photo of these inclusions is shown in Figure 5.3.6.1.

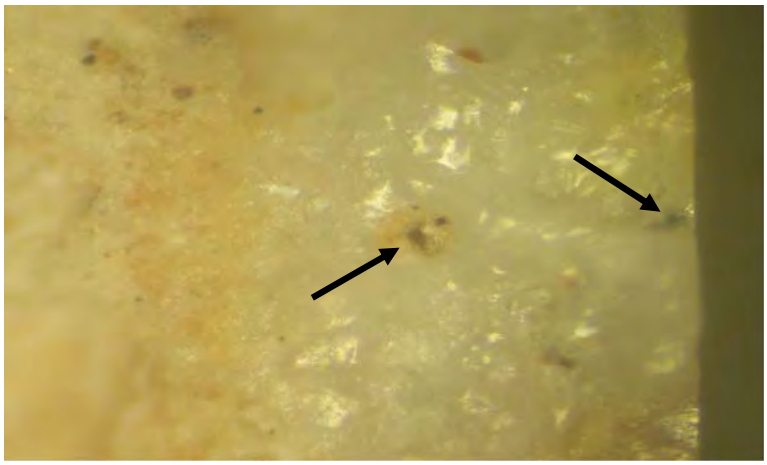

Figure 5.3.6.1. Amorphous carbon inclusions found in the glaze and presumed to be contamination that occurred during the manufacturing process. This photo was acquired with an Olympus camera mounted on top of the microscope using a 50X objective lens

5.4 Implications for restoration and preservation

The valuable information obtained from the study of the Citadel tile shard could be used for purposes of restoration and preservation of the Citadel itself. First, all the

pigments that were used have been positively identified. Secondly, the composition of the body of the tile has been determined, based on its major components. The direction of research for additional information to assist in the restoration process should include, among others, the manufacturing recipes of that time (~ 1615) for the various pigments and body material, and the raw material supply for the specific components (glaze, body or pigment).

5.5 Conclusion

The characterisation of the pigments and body of the tile shard from the Citadel of Algiers was accomplished by using micro-Raman spectroscopy as the major technique, complemented by powder X-ray diffraction (XRD) and energy-dispersive X-ray spectrometry(EDX). The results reveal a rich variety of pigments which include the newly rediscovered ternary yellow pigment ($Pb_2SnSbO_{6.5}$), Naples yellow ($Pb_2Sb_2O_7$), lead (II) stannate (Pb_2SnO_4), rosiaite ($PbSb_2O_6$), cassiterite (SnO_2) and cobalt blue ($CoAl_2O_4$).

The body of the tile is composed largely of hematite (α-Fe_2O_3), maghemite (γ-Fe_2O_3), magnetite (Fe_3O_4), quartz (α-SiO_2), glassy silica and traces of calcite ($CaCO_3$) and amorphous carbon.

The accumulated chemical information may be used in conjunction with information on preparation and raw material sources to design an appropriate restoration and conservation response programme for these ancient tiles. Micro-Raman spectroscopy proved to be very useful in pigment characterisation when used in conjunction with complementary techniques such as XRD and EDX.

5.6 References

1. Kock, L.D. and de Waal, D. *Spectrochim Acta Part A*. 2008, **71**, 1348.
2. De Waal, D. Tile shard donated for Raman Spectroscopy studies in the Department of Chemistry, University of Pretoria. 2006.
3. Clark, R.J.H., Cridland, L., Benson, M., Kariuki, K.D.M., Harris, D.M. and Withnall, R. *J. Chem. Soc. Dalton Trans*. 1995.
4. Kühn, H. In: *Artists Pigments*', Vol. 2, A. Roy (ed.), Oxford, Oxford University Press, 1994.
5. Martin, E. and Duval, A.R. *Stud. Conserv*. 1990, **35**, 117.
6. Wainwright, N.M., Taylor, J.M. and Harley, R.D. In: *Artists' Pigments,* Vol. 1, R.L. Feller (ed), Cambridge, Cambridge University Press, 1986, p 219.
7. Ruiz-Moreno, S., Perez-Pueyo, R., Gabaldon, A., Soneira, M-J. and Sandalinas, C. *J. Cultural Heritage.* 2003, **4**, 309s.
8. Sandalinas, C. and Ruiz-Moreno, S. *Studies in Conservation.* 2004, **49,** 41.
9. Sandalinas, C., Ruiz-Moreno, S., Lopez-Gill, A. and Miralles, J. *J. Raman Spectrosc*. 2006*,* **37**, 1146.
10. Cascales, C., Alonso, J.A. and Rasines, I. *J. Mater. Sci. Lett*. 1986, **5**, 675.
11. Dik, J., Hermens, E., Peschar, R. and Schenk, H. *Archaeometry.* 2005, **47**, 593.
12. Edwards, H.G.M. *J. Raman Spectrosc*. 2004, **35**, 656.
13. Katiyar, R.S. and Krishnan, R.S. *Phys. Lett*. 1967, **25A,** 525**.**
14. Ocaña, M., Serna, C.J., Garcia-Ramos, J.V. and Matijević, E. *Solid State Ionics.* 1993, **63**, 170.
15. Yu, K.N., Xiong, Y., Liu, Y. and Xiong, C. *Phys. Rev*. 1997, **55**, 2666.
16. Colomban, P., Milande, V. and Le Bihan, L. *J. Raman Spectrosc*. 2004, **35**, 527.

17. Colomban, P., de Laveaucoupet, R. and Milande, V. *J. Raman Spectrosc*. 2005, **36**, 857.
18. Christesen, S., Gonser, K., Lochner, J.M., Sedlacek, A., Chyba, T., Sink, D., Pendell Jones, J., Corrado, B. and Slaterbeck, A. *UV Raman Detection Of Chemical Agents*. Naval Surface Warfare Center, Dahlgren, Virginia USA, 2004.
19. Long, D.A. *The Raman Effect.* New York, Wiley, 2002.
20. Pettinger, B., Ren, B., Picardi, G., Schuster, R. and Ertl, G. 2005, **36**, 541.
21. De Waal, D. *Asian Chem. Lett*. 2004, **8**, 57.
22. De Faria, L.A., Silva, S.V. and de Oliviera. M.T. *J. Raman Spectrosc*. 1997, **28,** 873.
23. Burgio, L. and Clark, R.J.H. *Spectrochim. Acta.* 2001, **57**, 1491.
24. Mortimore, J.L., Marshall, L-JR., Almond, M.J., Hollins, P. and Matthews W. *Spectrochim. Acta.* 2004, **60A**, 1179.
25. Legodi, M.A. and de Waal, D. *Spectrochim. Acta Part A.* 2007*,* **66,**135.
26. Orlianges, J.C., Champeaux, C., Catherinot, A., Merle, Th. and Angleraud, B. *Thin Solid Films.* 2004, **453**, 285.
27. Nakamoto, K. *Infrared and Raman Spectra of Inorganic and Coordination Compounds*, Part A, Theory and Applications in Inorganic Chemistry, New York, Wiley, 1997, p 138.
28. Mammone, J.F., Nicol, M. and Sharma, S.K. *J. Phys. Chem. Solids.* 1981, **42**, 379.
29. Ristić, M., Ivanda, M., Popović, S. and Musić, S. *J. Non-Crystall. Solids.* 2002, **303,** 270.
30. Kawashima, Y. and Katagiri, G. *Phys. Rev*. 1995, **B14**, 52.

Appendix 5.1

EDX data: Yellow section of Citadel tile

Elements	Wt% Sec 1	Wt% Error	Wt% Sec 2	Wt% Error	Wt% Sec 3	Wt% Error	Wt% Sec 4	Wt% Error	Wt% Sec 5	Wt% Error	Wt% Sec 6	Wt% Error	Wt% Sec 7	Wt% Error
Na	0.45	0.08	0.34	0.08	0.19	0.07	0.32	0.08	0.17	0.06	0.26	0.08	0.18	0.07
Mg	0.33	0.06	0.15	0.06	0.12	0.06	0.18	0.06	0.04	0.06	0.08	0.06	0.16	0.05
Al	3.00	0.13	2.43	0.12	2.08	0.12	2.59	0.12	1.77	0.11	2.22	0.11	1.98	0.11
Si	22.48	0.21	22.05	0.21	22.47	0.20	21.61	0.20	21.85	0.19	20.88	0.19	17.04	0.17
P	0.48	0.08	0.20	0.08	0.14	0.08	0.26	0.08	0.00	0.00	0.14	0.07	0.15	0.07
S	0.00	0.00	0.00	0.00	0.00	0.00	0.00	0.00	0.00	0.00	0.00	0.00	0.00	0.00
Cl	0.41	0.16	0.58	0.16	0.62	0.15	0.53	0.15	0.28	0.15	0.30	0.15	0.10	0.14
K	3.99	0.16	3.28	0.23	3.17	0.16	4.03	0.15	2.90	0.14	3.44	0.21	2.45	0.03
Ca	4.12	0.17	1.69	0.14	1.64	0.15	2.35	0.14	1.41	0.13	1.57	0.13	0.87	0.12
Mn	0.16	0.17	0.09	0.17	0.00	0.00	0.07	0.17	0.03	0.15	0.00	0.00	0.08	0.15
Fe	1.49	0.19	1.05	0.19	2.33	0.19	1.02	0.18	0.96	0.17	0.75	0.17	3.00	0.18
Co	0.00	0.00	0.26	0.20	0.15	0.19	0.00	0.00	0.32	0.19	0.14	0.19	0.00	0.00
Cu	0.14	0.26	0.17	0.26	0.29	0.25	0.38	0.25	0.31	0.25	0.20	0.23	0.24	0.23
Pb	59.36	3.54	61.80	3.56	58.15	3.50	60.47	2.34	63.78	2.28	64.65	3.35	67.71	2.19
Ti	0.00	0.00	0.04	0.11	0.05	0.10	0.01	0.13	0.00	0.00	0.00	0.00	0.11	0.11
Cr	0.00	0.00	0.00	0.00	0.00	0.00	0.00	0.00	0.00	0.00	0.10	0.11	0.09	0.11
Sn	0.54	0.60	2.05	0.50	3.46	0.57	1.20	0.47	2.56	0.44	1.37	0.46	0.69	0.40
Sb	3.06	0.81	3.82	0.37	5.15	0.76	4.59	0.36	3.21	0.34	3.91	0.34	4.53	0.31
Ba	0.00	0.00	0.00	0.00	0.00	0.00	0.41	0.31	0.42	0.24	0.00	0.00	0.62	0.28